

RESISTIVE WALL WAKE EFFECT OF A GROOVED VACUUM CHAMBER *

Karl L.F. Bane and Gennady Stupakov

Stanford Linear Accelerator Center, Stanford University, Stanford, CA 94309, USA

Abstract

To suppress the emission of secondary electrons in accelerators with positively charged beams (ions or positrons) it has been proposed to use a vacuum chamber that is longitudinally grooved (or, equivalently, one can say finned). One consequence of having such a chamber in an accelerator is an increased resistive wall impedance. In this paper, we calculate the resistive wall impedance of one such finned chamber, planned to be used in experimental studies of secondary emission suppression at SLAC. For rectangular fins, we use an analytical method based on a conformal mapping approach; we compare the results with a numerical solution of the field equation. We also numerically compute the impedance for rounded fins (as will be used in the SLAC experiment) and analyze how the impedance depends on geometric properties of the fins.

INTRODUCTION

In high-current storage rings with positively charged beams, such as the positron damping ring of the International Linear Collider (ILC) project, the electron cloud effect can seriously limit performance. One mitigating measure that has been proposed is to replace the flat surface of the vacuum chamber with one containing longitudinal grooves. Such grooves reduce the secondary emission of electrons which, in turn, suppresses the electron cloud effect [1–3]. A grooved vacuum chamber, however, will have an increased resistive wall impedance, which will tend to reduce the threshold to other instabilities, such as the multi-bunch (transverse) beam instability. In this report we calculate the increase in resistive wall impedance due to the grooves.

More specifically, in this report we consider a grooved (or it can be described as finned) vacuum chamber of period p and fin thickness t (see sketch on Fig. 1a). For the grooved chamber proposed for a SLAC experiment [4]: $p = 2.82$ mm, $t = 0.56$ mm, fin depth $d = 4.57$ mm, and beam pipe radius $a = 55.1$ mm; the fin tips are rounded and have a semi-circular profile.

The resistive wall wake will be increased by a scale factor when compared to that of a flat pipe surface. In this report we first find this factor for the case of rectangular fins using an analytical approach that employs Schwartz-Christoffel transformations. Note that a similar approach has been applied to finding fields of periodic structures *e.g.*

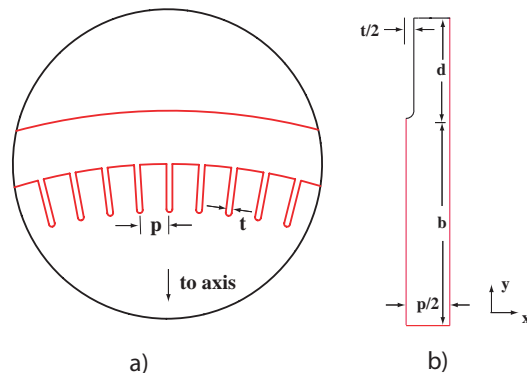


Figure 1: a)—detail of the grooved vacuum chamber wall; dimensions shown are period p and fin thickness t ; b)—geometry for the problem that is actually solved (for the case of rounded fin tips). The z axis points out of the page.

in [5]. Our result is then compared with that of a numerical calculation. Finally, the numerical method is applied to the round-tipped fin structure.

METHOD

The energy loss induced by the electromagnetic field inside the wall in the small skin depth approximation (a so called Leontovich boundary condition [6]) is proportional to the square of the magnetic field on the metal surface. Therefore, the enhancement η of the resistive wall wake effect (both transverse and longitudinal) for the finned beam pipe, compared to a normal beam pipe, can be written as

$$\eta = \frac{\int H^2 ds}{H_0^2 p}, \quad (1)$$

where H is magnetic field on the surface of the metal, H_0 the magnetic field in the case of a flat (non-grooved) surface, and integration follows the grooved surface over one period in a plane of constant z (the z axis points out of the page in Fig. 1). The magnetic field can be represented as $\mathbf{H} = \hat{z} \times \nabla \psi$, with \hat{z} the unit vector in z and the magnetic potential ψ satisfying the two-dimensional Laplace equation $\nabla^2 \psi = 0$. Note that using the Laplace equation for the magnetic field is valid for frequencies ω such that $c/\omega \ll p$; for our parameters $p \sim 3$ mm this means $\omega \lesssim 2\pi \cdot 10^{11}$ Hz.

Neglecting the curvature due to the pipe radius a (which is valid if a is much larger than the fin depth d) and using

* Work supported by the Department of Energy, contract DE-AC02-76SF00515

the symmetry of the problem, we actually solve the Laplace equation for the geometry shown in Fig 1b, which covers half of the period $p/2$ and extends beyond the tip of the fins (toward the center of the pipe) by some distance b . The exact value of b is not important as long as $b \gg p$. The boundary condition for the magnetic field \mathbf{H} is that it is tangential on the surface of the metal, as well as at the bottom horizontal line (where $H \equiv H_0$), and it is perpendicular to the vertical lateral boundaries. In terms of the potential ψ this means that $\psi = 0$ on the metal surface, $\psi = \text{const}$ at the bottom and $\partial\psi/\partial n = 0$ at the vertical boundaries.

ANALYTICAL APPROACH

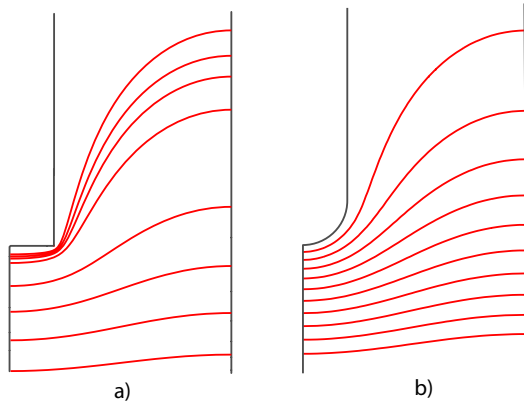


Figure 2: Magnetic field lines in the vicinity of a fin with rectangular (a) and rounded (b) fin tips.

We first calculate the enhancement factor η for the case of rectangular fins. In this case the solution $\psi(x, y)$ can be obtained with the help of conformal mapping using the Schwartz-Christoffel integral [7]. We introduce the complex variables $w = \psi + i\phi$ and $u = -y - ix$, with ψ being the magnetic potential, ϕ an auxiliary function and x and y the rectangular coordinates. The signs in the relation $u = -y - ix$ correspond to the coordinate system shown in Fig. 1b, with the origin located in the upper right corner. Omitting the derivation, we present here the final result of the conformal map $u(w)$:

$$u = 2\sqrt{\frac{\zeta - A}{(A - B)(A - \zeta)}} \left[(B - A)F\left(\mu, \frac{B(A - 1)}{(A - B)}\right) + (1 - B)\Pi\left(\frac{A - 1}{A - B}, \mu, \frac{B(A - 1)}{(A - B)}\right) \right], \quad (2)$$

with

$$\mu = \sin^{-1} \left(\sqrt{\frac{(A - B)(1 - \zeta)}{(A - 1)(B - \zeta)}} \right), \quad (3)$$

and

$$\zeta = \frac{1}{4}e^{-w} (1 + e^w)^2. \quad (4)$$

Here $F(\mu, \tau)$ is the elliptic integral of the first kind, $\Pi(\xi, \mu, \tau)$ is the incomplete elliptic integral, and A and B

are numbers related to the geometric parameters p , t and d . The real part of the inverse function $u^{-1}(w)$ gives the potential ψ as a function of coordinates x and y . We find that for the values of p , t and d given above, $A = 0.36$ and B is very close to unity, $1 - B = 5 \cdot 10^{-6}$. The calculation of the enhancement factor gives $\eta = 1.7$.

The magnetic field lines in the vicinity of a fin calculated with the map Eqs. (2)-(4) are shown in Fig. 2a. In Fig. 3 we plot H^2 as function of distance along the metallic surface s (the red curve). The point $s = 0$ is at the center of the bottom surface of the fin (the center of the tip), $s = s_c = 0.28$ mm is the corner where the bottom (horizontal) and vertical fin surfaces meet. We note that, at the corner, there is the expected singularity $H^2 \sim |s - s_c|^{-2/3}$ (see *e.g.* [8]).

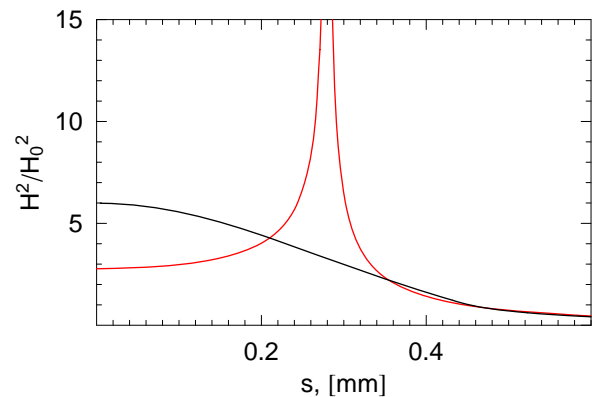


Figure 3: Normalized H^2 as function of distance along the metallic surface s , for the the vacuum chamber with flat fin tips (red color) and for rounded fin tips (black curve). The point $s = 0$ is at the bottom of the fin (the tip) in the midplane.

NUMERICAL SOLUTION

Laplace's equation for the grooved vacuum chamber was also solved using Matlab's Partial Differential Equation toolbox. This is a 2D finite element, partial differential equation solver. For the calculation we took $b = 10$ mm, and used $\sim 3 \cdot 10^5$ mesh points.

We first performed the calculation for the case of rectangular fins. The numerically obtained H^2 on the surface of the fins is in good agreement with the analytical solution of above; in fact, when plotted over the range of Fig. 3, the two solutions are nearly indistinguishable. The finite element program, however, cannot produce the proper singular behavior, and the discrepancy becomes apparent when one zooms in very close to the corner. Consequently, the numerically obtained $\eta = 1.46$ does not agree with the analytical value of 1.7, and is 15% less, than the analytical solution.

The numerical calculation was repeated for the case of rounded fins. Magnetic field lines in the vicinity of a rounded fin are shown in Fig. 2b. The normalized H^2 on

the fin surface is given in Fig. 3 (the black curve). Here the maximum field is at the very tip of the fins and there is no singularity. Note that, when moving upward along the tip surface (into the groove), the round and rectangular fin solutions asymptotically converge. The enhancement factor for rounded fins $\eta = 1.47$, 14% less than for rectangular fins.

We have earlier noted that a does not influence our result; for $d \gtrsim p$, d also does not influence the result. In this case we are left with only one free parameter, (t/p) . In Fig. 4 we plot the numerically obtained η (for rounded fins) as function of t/p . The central point on this plot corresponds to the numerical values of p and t used above. We see that η slowly increases as t/p is reduced.

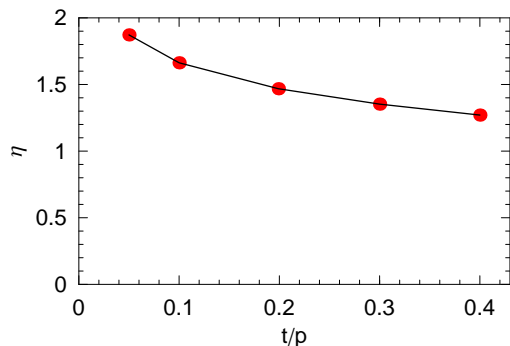


Figure 4: For the vacuum chamber with rounded fin tips: the enhancement factor η as function of t/p (the plotting symbols).

CONCLUSION

We have studied the effect on the strength of the resistive wall impedance of using a round beam pipe with longitudinal grooves (or one can say fins), something that is being considered to mitigate the electron cloud effect in storage rings. For the case of flat-tipped fins we have found an analytical solution of magnetic field enhancement using conformal mapping techniques. The calculation was repeated using a numerical partial differential equation solver. Comparison of the surface magnetic field for the two solutions found excellent agreement (except very close to a singularity, where the numerical method fails). The numerical approach was repeated for rounded fin tips, for various values of fin thickness over groove period. For the specific grooved chamber proposed for a SLAC experiment, we find the impedance enhancement factor ~ 1.5 .

ACKNOWLEDGEMENT

The authors thank M. Pivi for introducing us to this problem, and for providing the geometry for the grooved chamber being built at SLAC.

REFERENCES

- [1] V. Baglin, J. Bojko, O. Gröbner, B. Henrist, N. Hilleret, C. Scheuerlein, and M. Taborelli, in *Proc. European Particle Accelerator Conference, Vienna, 2000* (2000).
- [2] A. A. Krasnov, *Vacuum* **73**, 195 (2004).
- [3] G. Stupakov and M. Pivi, *Suppression of the effective secondary emission yield for grooved metal surface*, Preprint SLAC-TN-04-045, SLAC (2004).
- [4] Private communication by M. Pivi, SLAC, Jan. 2006.
- [5] Y. A. Tsarin, *Microwave and Optical Technology Letters* **20**, 57 (2000).
- [6] L. D. Landau and E. M. Lifshitz, *Electrodynamics of Continuous Media*, vol. 8 of *Course of Theoretical Physics* (Pergamon, London, 1960), 2nd ed., (Translated from the Russian).
- [7] R. V. Churchill and J. W. Brown, *Complex variables and applications* (McGraw-Hill, 1989), 5th ed.
- [8] R. Mittra and S. W. Lee, *Analytical techniques in the theory of guided waves* (McMillan, 1971).